Carpet anti-cloak based on transformation optics

Xuan Liu (刘 萱), Luoning Zhang (张洛宁), Jing Zhou (周 静)*, Jinwei Shi (石锦卫), Zhaona Wang (王兆娜), and Dahe Liu (刘大禾)

Applied Optics Beijing Area Major Laboratory, Department of Physics, Beijing Normal University, Beijing 100875, China

**Corresponding author: jzhou@bnu.edu.cn*

Received July 10, 2014; accepted October 24, 2014; posted online November 28, 2014

We propose a scheme for carpet anti-cloak based on the transformation optics. An anti-cloak layer is designed, which can make the external electromagnetic waves break the carpet cloak shielding. The external electromagnetic waves can be detected under the carpet cloak, while not affecting the role of carpet cloak of stealth. The Jacobian transformation tensor is calculated by numerically solving the Laplace equations with proper boundary condition. Thus, it is possible to design the anti-cloak layer of irregular shape. The simulation results demonstrate the feasibilities and flexibilities of the structure. Design details and full-wave simulation results are provided.

OCIS codes: 160.3918, 230.0040, 000.3870.
doi: 10.3788/COL201412.121601.

Transformation optics (TO) and electromagnetic invisibility cloaking have been attracting extreme interest both in theory and in experiment since Pendry *et al.* designed a cloak using TO[1] and Leonhardt developed an invisibility device by conformal transformation[2] simultaneously in 2006. Numerical calculations using perfectly matched layers for the absorption of electromagnetic waves[3] demonstrated the properties of the invisibility cloaking. The theory of TO is based on the form invariance of Maxwell's equations in different coordinate systems[4]. The scheme of the electromagnetic invisible cloak was first experimentally confirmed in 2006[5]. Now supported by the advent of metamaterials[6–10], TO has attracted great deal of attention in many electromagnetic applications[11–14]. In order to avoid the parameters singularities of the spherical or cylindrical cloak and make the parameters isotropic, a carpet cloak was proposed to make the cloaked objects look like a flat perfect conductor (PC) surface[15]. This idea has been experimentally demonstrated at both microwave[16] and optical[17,18] frequencies. However, the cloak can only hide objects, but cannot watch outside because the external electromagnetic waves cannot penetrate the cloak layer. In 2008, the idea of anti-cloak was proposed[19], which could partially defeat the cloaking effect by making the external electromagnetic wave penetrate through the invisibility cloak media. Then this concept was applied for the spherical and/or cylindrical cloaks in Refs. [20–24]. The objects placed inside the cloaked area can receive the external wave information and the waveform of the external electromagnetic waves remains unchanged. Thus, the objects are still invisible for the viewer outside the cloak. On the other hand, in Ref. [25], the scheme of carpet anti-cloak via a rectangular anti-cloak layer was proposed. To the best of our knowledge, the carpet anti-cloak with irregular shape has not been reported, which is an interesting and more general structure. In this letter, we propose a scheme for the carpet anti-cloak with irregular shape based on TO. The material parameters of the anti-cloak are designed by numerically solving Laplace's equation because the space transformation of irregular shape is complex and difficult to analytically express.

The electromagnetic invisibility carpet cloak is schematically shown in Fig. 1. As shown in Fig. 1(a), the carpet cloak layer is constructed by compressing the sliding edge d attached to the ground plane to the edge b, leaving enough space for an object to be concealed. Figure 1(b) shows the numerical simulation result. A TE polarized Gaussian beam approaches the cloak at

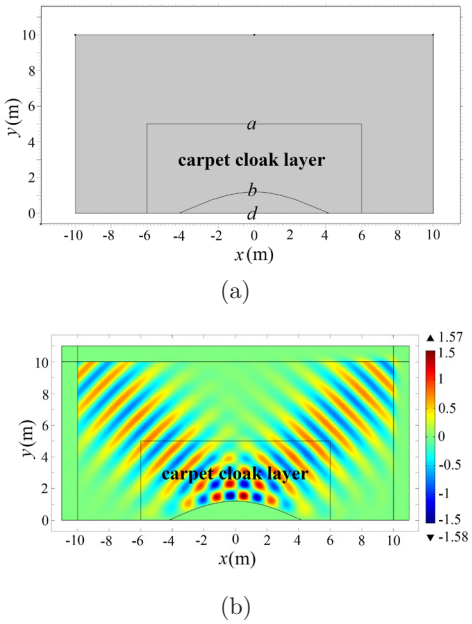

Fig. 1. (a) Geometry of the carpet cloak and (b) distribution of the electric field of the carpet cloak.

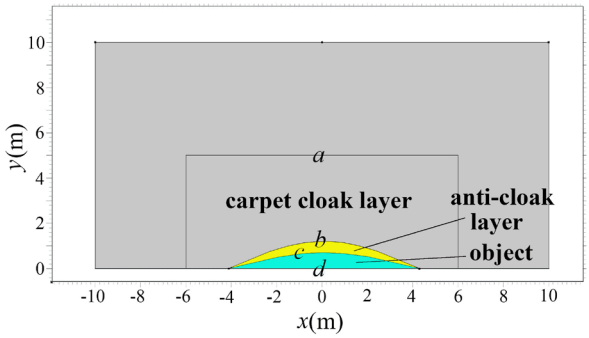

Fig. 2. Geometry of the carpet anti-cloak.

45° with respect to the ground plane. Obviously, the electric field distribution of the reflected beam outside the cloak has the appearance of that reflected from a flat plate. Here the bottom edge of the cloak is highly reflective as realized by PC boundary condition. On the other hand, the incident wave cannot get into the cloaked area and consequently cannot be detected by the cloaked object.

In order to make the external electromagnetic wave penetrate the carpet cloak layer and keep the inner object being invisible from the outside, we propose to embed a complementary medium layer between the cloak layer and the object. As shown in Fig. 2, the bottom blue area is the object and the middle yellow layer is the complementary medium, which can be called anti-cloak layer.

This anti-cloak layer is constructed by the space transformation that compresses the ground plane d to the bottom edge of the cloak b, while keeping the curved surface c unchanged. Then the external electromagnetic wave reaches the boundary b just like touching the flat ground plane d. In this case, the external electromagnetic wave can penetrate the cloak region and will be detected by the object.

It is known from the theory of TO that the permittivity and permeability in the transformed space are given by[26]

$$\varepsilon' = \frac{A\varepsilon A^{\mathrm{T}}}{|A|}, \quad \mu' = \frac{A\mu A^{\mathrm{T}}}{|A|}, \tag{1}$$

where ε and μ are the permittivity and permeability of the original flat space x, and ε' and μ' are that of the transformed or distorted space $x'(x)$. $\boldsymbol{A}$ is the Jacobian tensor representing the space transformation. The components of $\boldsymbol{A}$ are determined by

$$A_{ij} = \frac{\partial x_i'}{\partial x_j}. \tag{2}$$

Thus, A_{ij}describes the geometrical distortion from the original space to the transformed space. Obviously, the values of ε' and μ' are related to that of ε and μ. Assume the permittivity and permeability of the object under the cloak are $\varepsilon_{\mathrm{ob}}$ and μ_{ob}. It can be seen from Eq. (1)

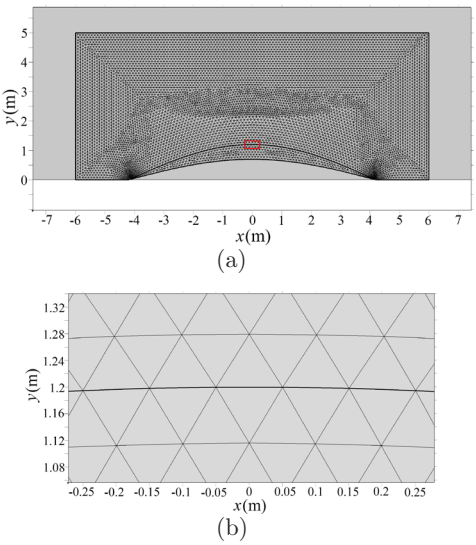

Fig. 3. (a) Meshed grids of transformed regions for calculating the Jacobian tensor A by the PDE module of COMSOL Multiphysics and (b) enlargement of the red box in (a).

that the material parameters of the anti-cloak layer should be

$$\varepsilon'_{\mathrm{anti}} = \frac{A\varepsilon_{\mathrm{ob}}A^{\mathrm{T}}}{|A|}, \quad \mu'_{\mathrm{anti}} = \frac{A\mu_{\mathrm{ob}}A^{\mathrm{T}}}{|A|}. \tag{3}$$

It can be derived that the signs of $\varepsilon'_{\mathrm{anti}}$ and μ'_{anti} are opposite to that of $\varepsilon_{\mathrm{ob}}$ and μ_{ob} because the used space transformation is a folded one[27].

As expressed in Eq. (2), the element values of A are determined by the space coordinate transformation. Nevertheless, the used space transformation for the anti-cloak layer is difficult to be analytically expressed because the shapes of the curved surfaces b and c are irregular. Supported by the well-developed numerical calculation software, this transformation scheme can be realized by numerically solving Laplace's equation with the proper boundary conditions[28,29]. We calculated the Jacobian tensor A by the partial differential equation (PDE) module of COMSOL Multiphysics. In the calculation, the transformed regions were meshed with triangular grids as shown in Fig. 3(a). The maximum element size is 0.1 m. Figure 3(b) shows the enlargement of the red box in Fig. 3(a). The numbers of degrees of freedom are 56662 for the carpet cloak layer and 20642 for the anti-cloak layer.

In order to verify the scheme proposed above, we make the numerical simulation with RF module of COMSOL Multiphysics. Without loss of generality, a TE polarized Gaussian beam is taken as incident wave, which propagates at 45° relative to the ground plane. First, we consider a carpet cloak without an anti-cloak layer with the boundary b of the continuous condition. As shown in Fig. 4(a), the incident wave with frequency of 2×10^8 Hz enters into the cloaked region, and is scattered back randomly. This means that the object

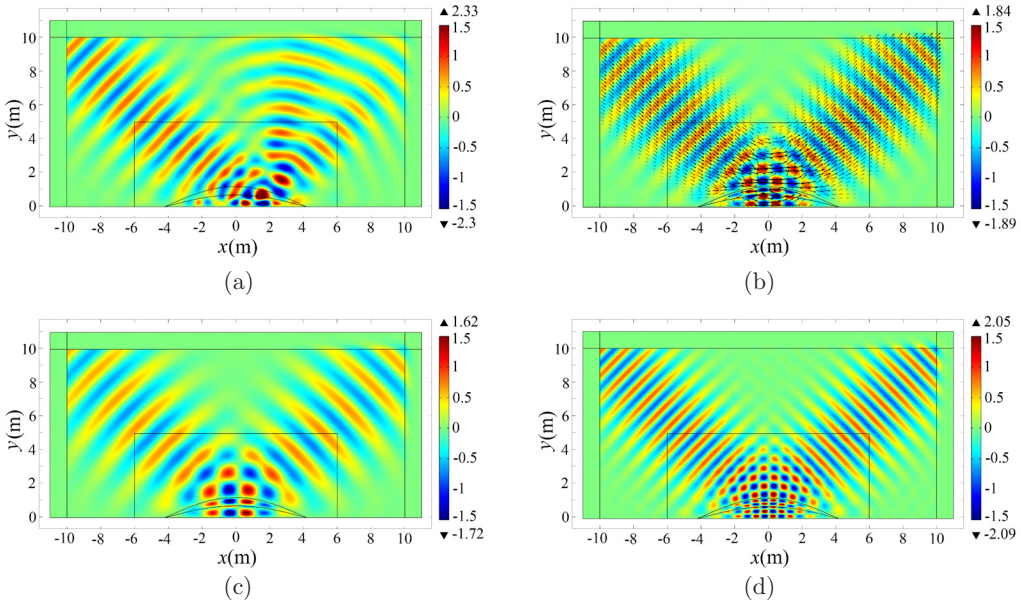

Fig. 4. (a) Distribution of the electric field of a carpet cloak with its bottom of continuous boundary. (b), (c), and (d) are the field distributions around the carpet anti-cloak with the wave frequencies of 2×10^8, 1.5×10^8, and 3×10^8 Hz, respectively. The parameters of the object under the cloak are $\varepsilon_{ob}=2$ and $\mu_{ob}=2$.

becomes visible and the cloak is partially broken. Then we simulated the field property of the invisible cloak with the anti-cloak layer. Figure 4(b) shows the calculated distribution of the electric field (with the logarithmic Poynting vector map superimposed). It can be seen that the invisibility cloaking is recovered, whereas the external electromagnetic wave gets into the cloaked area. The Poynting vector distribution shows that the power circulates in the cavity formed by the anti-cloak layer and the inner object, which via the vanishingly small coupling through the cloaked layer is able to restore a modal field. This is similar to the cylinder anti-cloak in Ref. [20]. Figures 4(c) and (d) show the simulated field distributions for the wave frequencies of 1.5×10^8 and 3×10^8 Hz, respectively.

By calculation, the object's parameters are found to be $\varepsilon_{ob}=2$ and $\mu_{ob}=2$. The parameters of ε'_{anti} and μ'_{anti} for the anti-cloak layer are calculated by Eq. (3). Figure 5 shows the space distributions of the nonzero components of ε'_{anti} and μ'_{anti}. It is found that all the components are finite and small.

The scheme proposed above also applies to the object consisting of absorption media. In order to consider the absorption case, we set $\varepsilon_{ob}=2+2i$ and $\mu_{ob}=1$ as example. When the boundary b in the carpet cloak is with the continuous condition, the object becomes visible as shown in Fig. 6(a). When the anti-cloak layer is embedded between the cloak and the object, the distributions of electric fields are as presented in Fig. 6(b). It is shown that the distribution of the electric field outside the carpet cloak stays the same as that reflected from the flat ground plane, demonstrating that the property of the invisibility cloaking reserves, whereas the external electromagnetic waves can be detected under the anti-cloak layer.

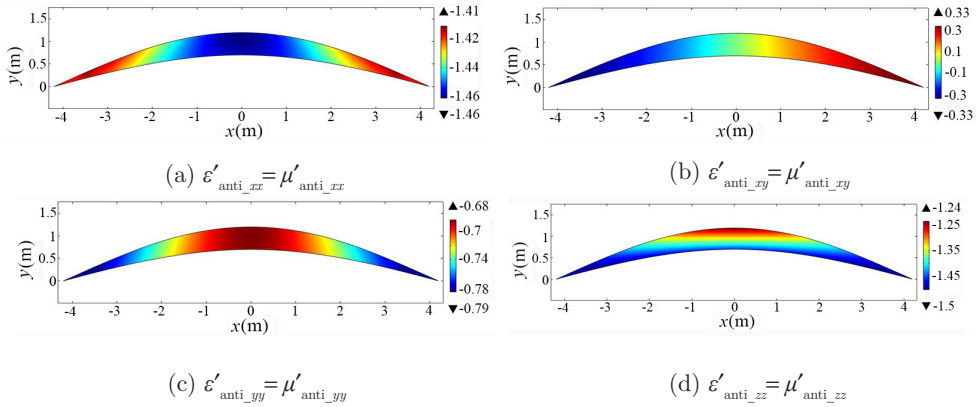

Fig. 5. Distributions of the material parameters of the anti-cloak layers, with $\varepsilon_{ob}=2$ and $\mu_{ob}=2$.

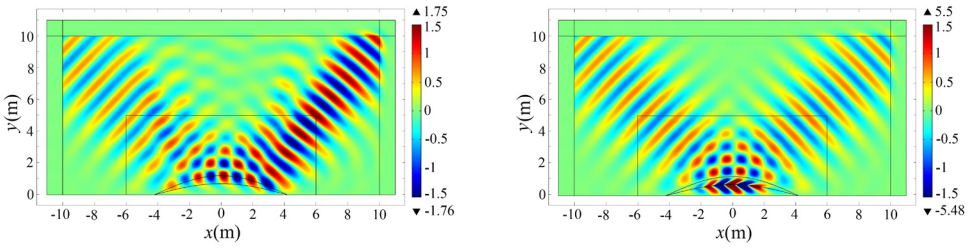

(a) (b)

Fig. 6. (a) Electric field distribution of a carpet cloak with its bottom of continuous boundary and (b) field distribution around the carpet anti-cloak. The parameters of the object are $\mu_{ob}=1$ and $\varepsilon_{ob}=2+2i$.

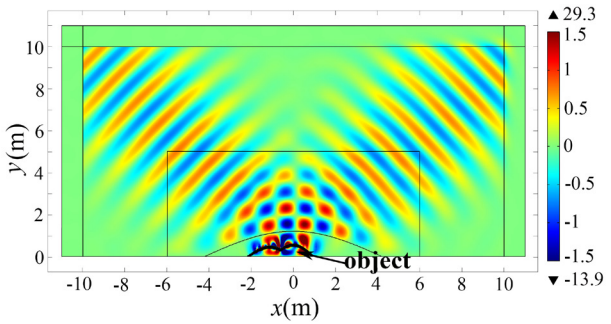

Fig. 7. Electric field distribution of a carpet anti-cloak with irregular shape.

In order to demonstrate that the shape of the anti-cloak layer can be irregular, we present another example in Fig. 7. The shape of the object is irregular and different from the previous one. The incident wave and the optical parameters of the object are same as that in Fig. 4(b). The property of the anti-cloak layer remains unchanged.

In conclusion, a carpet anti-cloak is proposed based on the TO. Full-wave numerical calculations demonstrate that the external electromagnetic waves can be detected under the carpet cloak, while not affecting the stealth character of the carpet cloak. With the help of numerically solving Laplace's equation, the anti-cloak layer of irregular shape can be designed.

This work was financially supported by the National Natural Science Foundation of China under Grant No. 61275130. The authors also appreciate the help in numerical simulations provided by Prof. Zhengming Sheng and Dr. Jun Zheng in Shanghai Jiaotong University.

References

1. J. B. Pendry, D. Schurig, and D. R. Smith, Science **312,** 1780 (2006).
2. U. Leonhardt, Science **312,** 1777 (2006).
3. J. Berenger, J. Comput. Phys. **114,** 185 (1994).
4. U. Leonhardt and T. G. Philbin, N. J. Phys. **8,** 247 (2006).
5. D. Schurig, J. J. Mock, B. J. Justice, S. A. Cummer, J. B. Pendry, A. F. Starr, and D. R. Smith, Science **314,** 977 (2006).
6. M. Kadic, T. Bückmann, R. Schittny, and M. Wegener, Rep. Prog. Phys. **76,** 126501 (2013).
7. M. Z. Ali, Chin. Opt. Lett. **10,** 071604 (2012).
8. Y. Chen, Y. Fang, S. Huang, X. Yan, and J. Shi, Chin. Opt. Lett. **11,** 061602 (2013).
9. R. Tsu and M. A. Fiddy, Photon. Res. **1,** 77 (2013).
10. J. Zhao, H. Zhang, X. Zhang, D. Li, H. Lu, and M. Xu, Photon. Res. **1,** 160 (2013).
11. H. Chen and C. T. Chan, Appl. Phys. Lett. **90,** 241105 (2007).
12. M. Rahm, D. Schurig, D. A. Roberts, S. A. Cummer, D. R. Smith, and J. B. Pendry, Photon. Nanostruct. Fundament. Appl. **6,** 87 (2008).
13. T. Yang, H. Y. Chen, X. D. Luo, and H. R. Ma, Opt. Express **16,** 18545 (2008).
14. J. Ng, H. Y. Chen, and C. T. Chan, Opt. Lett. **34,** 644 (2009).
15. J. Li and J. B. Pendry, Phys. Rev. Lett. **101,** 203901 (2008).
16. R. Liu, C. Ji, J. J. Mock, J. Y. Chin, T. J. Cui, and D. R. Smith, Science **323,** 366 (2009).
17. J. Valentine, J. Li, T. Zentgraf, G. Bartal, and X. Zhang, Nat. Mater. **8,** 568 (2009).
18. J. Renger, M. Kadic, G. Dupont, S. S. Aćimović, S. Guenneau, R. Quidant, and S. Enoch, Opt. Express **18,** 15757 (2010).
19. H. Chen, X. Luo, H. Ma, and C. T. Chan, Opt. Express **16,** 14603 (2008).
20. G. Castaldi, I. Gallina, V. Galdi, A. Alù, and N. Engheta, Opt. Express **17,** 3101 (2009).
21. G. Castaldi, I. Gallina, V. Galdi, A. Alù, and N. Engheta, Wave Motion **48,** 455 (2011).
22. I. Gallina, G. Castaldi, V. Galdi, A. Alù, and N. Engheta, Phys. Rev. B **81,** 125124 (2010).
23. A. Greenleaf, Y. Kurylev, M. Lassas, and G. Uhlmann, Phys. Rev. E **83,** 016603 (2011).
24. L. Li, F. Huo, Y. Zhang, Y. Chen, and C. Liang, Opt. Express **21,** 9422 (2013).
25. J. Zhao, D. Wang, R. Peng, Q. Hu, and M. Wang, Phys. Rev. E **84,** 046607 (2011).
26. G. W. Milton, M. Briane, and J. R. Willis, N. J. Phys. **8,** 248 (2006).
27. M. Kadic, S. Guenneau, S. Enoch, and S. A. Ramakrishna, ACS Nano **5,** 6819 (2011).
28. J. Hu, X. Zhou, and G. Hu, Opt. Express **17,** 1308 (2009).
29. X. Liu, X. Li, J. Zhou, Z. Wang, J. Shi, and D. Liu, Opt. Express **21,** 30746 (2013).